Carbohydrate Polymers 81 (2010) 213–218

Contents lists available at ScienceDirect

Carbohydrate Polymers

journal homepage: www.elsevier.com/locate/carbpol

Micellization and sustained drug release behavior of EC-*g*-PPEGMA amphiphilic copolymers

Junjun Tan[a,b], Yanxiang Li[a], Ruigang Liu[a,*], Hongliang Kang[a], Deqian Wang[a,b], Lin Ma[a,b], Wenyong Liu[a,b], Min Wu[a,b], Yong Huang[a,c,d,**]

[a] *State Key Laboratory of Polymer Chemistry and Physics, Beijing National Laboratory for Molecular Sciences, Institute of Chemistry, Chinese Academy of Sciences, Beijing 100190, China*
[b] *Graduate University, Chinese Academy of Science, Beijing 100039, China*
[c] *National Research Center of Engineering Plastics, Technical Institute of Physics and Chemistry, Chinese Academy of Sciences, Beijing 100190, China*
[d] *Laboratory of Cellulose and Lignocellulosics Chemistry, Guangzhou Institute of Chemistry, Chinese Academy of Science, Guangzhou 510650, China*

ARTICLE INFO

Article history:
Received 30 November 2009
Received in revised form 3 February 2010
Accepted 9 February 2010
Available online 7 March 2010

Keywords:
Ethylcellulose
Graft copolymer
Micelles
Drug release

ABSTRACT

The micellization and sustained drug release behavior of ethyl cellulose graft poly(poly(ethylene glycol) methyl ether methacrylate) (EC-*g*-PPEGMA) copolymers with well-defined structure were investigated by using pyrene as the fluorescent probe and model drug. It was found that the EC-*g*-PPEGMA copolymers have a low critical micelle concentration (CMC) at about 5×10^{-4} mg/mL. Drug loading experiments indicate that a low graft density of the copolymers corresponds to a higher drug loading efficiency and a higher loading capacity of drug in the micelles. The release rate of the loaded pyrene depends on both the length of the side chains and the loading capacity of pryene in the micelles. A shorter side chain of the copolymer and a higher ratio of the copolymer to the pyrene in the micelles correspond to a lower release rate. The self-assembly system shows a potential application in controlled drug delivery.
© 2010 Elsevier Ltd. All rights reserved.

1. Introduction

Cellulose is the most abundant renewable biomacromolecule in nature. Cellulose and its derivatives have the advantages of nontoxicity, biocompatibility, and biodegradability, and have been widely used in the fields of composites (CancheEscamilla, RodriguezTrujillo, HerreraFranco, Mendizabal, & Puig, 1997), water treatment (Guclu, Gurdag, & Ozgumus, 2003; Hebeish, Waly, Abdel-Mohdy, & Aly, 1997; Srivastava & Behari, 2006; Waly, Abdel-Mohdy, Aly, & Hebeish, 1998), drilling-mud additives (Zhang, Tan, & Li, 1999), microfiltration membranes (Rajam & Ho, 2006), separation (Yu, Fu, Zhao, Liu, & He, 2006), absorbent resins (Pourjavadi & Mahdavinia, 2005), flocculants (Biswal & Singh, 2006), solid–solid phase change materials (Li, Liu, & Huang, 2008), and drug delivery (Dong et al., 2008).

The micelle formation, as well as their application in the fields of medicine and biology has been investigated extensively in the past decade (Allen, Maysinger, & Eisenberg, 1999; Bajpai, Shukla, Bhanu, & Kankane, 2008; Discher & Eisenberg, 2002; Kabanov & Alakhov, 2002; Kataoka, Harada, & Nagasaki, 2001; Kwon & Okano, 1996; Kwon, 2003; Rapoport, 2007; Savic, Eisenberg, & Maysinger, 2006). As a drug carrier system, polymeric micelles prepared from amphiphilic graft or block copolymers are the potential candidate for the delivery of poorly water-soluble drugs, in which the hydrophobic core acts as a reservoir for poorly water-soluble drugs. Small polymeric micelles (<200 nm) also have the advantage of avoiding physical clearance by filtration in lungs and spleen or excretion through the kidneys. Moreover, the unique core-shell structure and nano-size can protect drugs from inactivation, prevent the sudden release in the physiological environment, and reduce the drug toxicity, which make them suitable as long-circulating drug carriers (Bian, Jia, Yu, & Liu, 2009). Compared with block copolymers, the micelle formed from amphiphilic graft copolymers, an important category of copolymers, are less studied (Chen, Ni, Wang, & Chen, 2008; Jun et al., 2006; Liu, Pramoda, Yang, Chow, & He, 2004; Liu, Lin, & Wu, 2008). The reason may be attributed to that traditional methods for the preparation of graft copolymers such as the free radical polymerization are not controllable and the resultant graft copolymers have a more complicated structure and are always mixed with homo-polymers.

In the last decade, the controllable/living radical polymerizations (CRP), such as atom transfer radical polymerization (ATRP)

* Corresponding author. Tel.: +86 10 82618573; fax: +86 10 62554670.
** Corresponding author at: State Key Laboratory of Polymer Chemistry and Physics, Beijing National Laboratory for Molecular Sciences, Institute of Chemistry, Chinese Academy of Sciences, Beijing 100190, China. Tel.: +86 10 82618573; fax: +86 10 62554670.
E-mail addresses: rgliu@iccas.ac.cn (R. Liu), yhuang@mail.ipc.ac.cn (Y. Huang).

0144-8617/$ – see front matter © 2010 Elsevier Ltd. All rights reserved.
doi:10.1016/j.carbpol.2010.02.017

and reversible addition fragmentation chain transfer polymerization (RAFT) (Moad, Rizzardo, & Thang, 2008; Roy, Guthrie, & Perrier, 2008; Wang & Matyjaszewski, 1995), have been developed and widely applied for the synthesis of homo- and block-polymers. The CRP methods have also been used for the preparation of cellulosic graft copolymers (Carlmark & Malmstrom, 2002; Fleet et al., 2008; Ifuku & Kadla, 2008; Kang et al., 2006; Kang, Liu, Liu, & Huang, 2008; Li, Liu, Liu, et al., 2008; Lindqvist et al., 2008; Meng et al., 2009; Ostmark, Harrisson, Wooley, & Malmstrom, 2007; Roy et al., 2008; Shen & Yong, 2004; Shen, Yu, & Huang, 2005; Shen, Yu, & Huang, 2006; Sui et al., 2008). The graft copolymerization of cellulose or cellulose derivatives with vinyl monomer by CRP was controllable and the resultant graft copolymers have a well-defined structure in graft density and side chain length. Thus the delicate hydrophilic/hydrophobic balance in a graft copolymer can be easily adjusted by changing the relative grafting density or side chains length (Li, Liu, Liu, et al., 2008; Wei, Cheng, Hou, & Sun, 2008; Yan et al., 2009). Such cellulosic amphiphilic graft copolymers have the ability to self-assemble to form micellar structure and may have the potential applications in controlled drug release system. However, investigation of the self-assembly and applications of such cellulosic graft copolymers is still limited.

In our previous work, we have synthesized a series of amphiphilic ethyl cellulose-*g*-poly(poly(ethylene glycol)$_{300}$ methyl ether methacrylate) (EC-*g*-PPEGMA) copolymers by ATRP (Li, Liu, Liu, et al., 2008). The graft copolymers have the ethyl cellulose (EC) backbone, which has the advantages of excellent hydrophobicility, plasticity, and good solubility in organic solvents, and has been used in controlled release coatings and microcapsules in the pharmaceutical industry. While the side PPEGMA chains is synthesized from poly(ethylene glycol) methyl ether methacrylate, a monomer derivative of poly(ethyleneglycol) that has potential biomedical applications due to the biocomapatiblity and nonadhesive nature to proteins and cells (Zhang et al., 2009). Such a graft copolymer structure offers the promising potential applications in controlled drug release system. However, the micellization behaviors and the drug loading and release behaviors of this graft copolymer have not been investigated. In this work, the drug loading and sustained release behaviors of the EC-*g*-PPEGMA with different graft density and graft length were investigated using pyrene as the fluorescence probe and model of the poor water-soluble drug. Our research aims to provide some positive information for the potential applications of cellulosic graft copolymers in drug delivery.

2. Experiment

2.1. Materials

Ethyl cellulose (EC) (Fluka, $M_w = 1.1 \times 10^5$ g/mol, $M_w/M_n = 3.6$, the degree of substitution of ethyl group is 2.5) was dried at 50 °C for 2 days before use. Poly(ethylene glycol) methyl ether methacrylate (PEGMA) (Aldrich, $M_n = 300$ g/mol) was purified by passing through a basic alumina column to remove the antioxidant inhibitor (MEHQ and BHQ). Pyrene (Alfa Aesar) was recrystallized from ethanol before use. Other chemicals and solvents are all analytical grade and used as received.

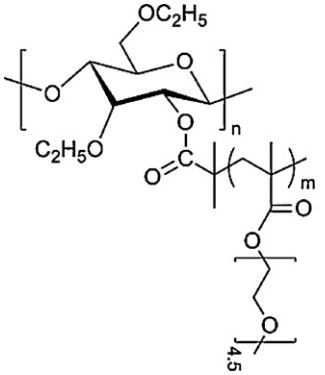

Scheme 1. The structural formula of EC-*g*-PPEGMA.

2.2. Preparation of EC-*g*-PPEGMA graft copolymers

EC-*g*-PPEGMA graft copolymers were synthesized by ATRP. The details of the synthesis procedure and characterization of the graft copolymers have been reported in previous work (Li, Liu, Liu, et al., 2008). For clarification, the structure of EC-*g*-PPEGMA copolymers is shown schematically in Scheme 1 and the details of the graft copolymers used in this work are listed in Table 1. In Table 1, the subscript the EC$_m$-*g*-PPEGMA$_n$ graft copolymers *m* and *n* represent the average number of side PPEGMA chain per glucose ring of EC backbone and the repeat unit of the side PPEGMA chain, respectively.

2.3. Micellization behavior of EC-*g*-PPEGMA probed by pyrene

The micellization behavior of the graft copolymer was researched using pyrene as fluorescent probe. The sample EC$_{0.04}$-*g*-PPEGMA$_{12.8}$ was selected for the investigation of the micellization behavior. Firstly the blank micelle solution of the graft copolymer was prepared by dialysis method. Typically, 10 mg EC-*g*-PPEGMA copolymers were dissolved in 5 mL THF with continuous stirring at room temperature overnight to obtain homogenous solution. The resultant solution was then transferred into a dialysis bag with a molecular weight cutoff of 3500 and dialyzed against distilled water for 24 h, during which the water was refreshed every 12 h to yield the micelle solution. The resultant concentration of EC-*g*-PPEGMA in the micelle solution was adjusted to 1 mg/mL. Secondly, known amount of pyrene in acetone was added into dry volumetric flask. After evaporation of the acetone, different amounts of copolymer micelle solutions were added to produce solution of various EC$_{0.04}$-*g*-PPEGMA$_{12.8}$ concentration with fixed pyrene con-

Table 1
The details of EC-*g*-PPEGMA copolymers and the loading efficiency and probe content of EC-*g*-PPEGMA micelles.

Sample	Graft density[a]	Side chain length[b]	W_{polym}/W_{py}[c]	Loading efficiency (%)	Probe content (%)
EC$_{0.15}$-g-PPEGMA$_{2.9}$	0.15	2.9	5:1	7.6	1.5
EC$_{0.15}$-g-PPEGMA$_{13.4}$	0.15	13.4	5: 1	4.3	0.6
EC$_{0.04}$-g-PPEGMA$_{6.6}$	0.04	6.6	5:1	17.7	4.4
			10:1	24.4	4.2
EC$_{0.04}$-g-PPEGMA$_{12.8}$	0.04	12.8	5:1	16.3	2.8
			10:1	28.3	4.1

[a] Average graft of side chains.
[c] The mass feeding ratio of graft copolymer to pyrene in the preparation of pyrene-loading micelles by dialysis chains per glucose ring of EC backbone.
[b] Average repeat units method.

centration at 5.0×10^{-7} mol/L. The fluorescence spectra of pyrene in $EC_{0.04}$-*g*-$PPEGMA_{12.8}$ were obtained at room temperature using a Cary Eclipse fluorescence spectrophotometer. The emission spectra was recorded at $\lambda_{ex} = 334$ nm and the excitation spectrum at $\lambda_{em} = 393$ nm.

2.4. Loading of pyrene into the EC-g-PPEGMA micelles

The incorporation of pyrene into polymeric micelles was carried out by the dialysis method as same as the blank micelle. Briefly, 10 or 20 mg EC-*g*-PPEGMA and 2 mg pyrene was dissolved in 5 mL THF to obtain homogenous solution and dialysized against water for 24 h during which the water was refreshed every 12 h. The resultant concentration of EC-*g*-PPEGMA copolymers in the resultant micelle solution was adjusted to 1 and 2 mg/mL, respectively.

The loading efficiency (E_L) and probe content (c_p) defined by Riley et al. (1999) as followed:

$$E_L(\text{wt.\%}) = \frac{w_p}{w_t} \times 100 \quad (1)$$

$$c_p(\text{wt.\%}) = \frac{w_p}{w_m} \times 100 \quad (2)$$

where w_p, w_t, and w_m are the mass of probe pyrene in micelles, total probe that used, and micelles, respectively. The loading efficiency and probe content was determined as follows. Generally, 2 mL pyrene-loading micelle solution was freeze-dried and weighted. Then the freeze-dried micelle was dissolved in THF and diluted to a certain volume. The content of pyrene was estimated by comparing the absorption intensity at $\lambda = 336.5$ nm on a Shimadzu UV-1601PC spectrophotometer. A calibration curve of the absorption intensity at $\lambda = 336.5$ nm as a function of pyrene content in THF in the linear range was used as the multipoint working curve. The EC-*g*-PPEGMA copolymer and the solvent have no obviously contribution to the UV–vis spectra and the background was subtracted. Averaged values of three experiments for each data were taken as the results.

The release behavior of the loading pyrene from the micelles was determined as follows. A dialysis bag with molecular weight cutoff of 14,000 g/mol containing 3 mL of the probe-loaded micelle aqueous solution was immersed in 500 mL phosphate buffer solution (PBS) (pH = 7.4) at 37 °C in a beaker with constant stirring, by which the pyrene can diffuse from the solution in the dialysis bag to the buffer solution through the dialysis bag. 50 μL micelle solution was taken from the dialysis bag at a certain time intervals and then diluted in 5 mL THF. The concentration of probe pyrene was determined by fluorescence spectra on a Cary Eclipse fluorescence spectrophotometer at $\lambda_{EX} = 334$ nm. Average value of three measurements was taken as the resultant data.

2.5. Characterization of the pyrene-loading micelles

The fluorescence spectrum of pyrene-loaded micelle was tested at $\lambda_{EX} = 334$ nm by Cary Eclipse fluorescence spectrophotometer. The hydrodynamic radius ($\langle R_h \rangle$) distribution of the pure micelles and pyrene-loaded micelles were determined by dynamic light scattering (DLS) performed on a commercial spectrometer (ALV/SP-150 equipped with an ALV-5000 multi-τ digital time correlator) and a solid-state laser (ADLS DPY 425II, output power about 400 MW at $\lambda = 632.8$ nm) as the light source. All the copolymer solutions were filtered through the Millipore Millex-FH nylon filter (0.45 μm) before measurements. All the experiments were carried out at a scattering angle of 90° at 25 °C. The hydrodynamic radius ($\langle R_h \rangle$) was obtained by the CONTIN program.

3. Results and discussion

3.1. Micellization behavior of EC-g-PPEGMA copolymers in aqueous solution

The onset of micellization in EC-*g*-PPEGMA copolymer was derived from steady-state fluorescent probe investigations using pyrene as the fluorescent probe. Pyrene is the most frequently used dye in fluorescence studies of labeled polymers (Winnik, 1993) and has been widely used in the studies on amphiphilic polymers, polymer chain dynamics, polymer/particle interfaces, polymer films, polymeric gels, and biological samples (Duhamel, 2005). The critical micelle concentration (CMC) of block copolymers in aqueous phase could be determined by the characteristic feature of pyrene excitation spectra (Kim et al., 2000). When the hydrophobic parts of the graft copolymers are associated together to form the core of the micelle, the pyrene molecules preferably locate inside the hydrophobic inner core, resulting in the red shift of the characteristic band of pyrene excitation spectra. Fig. 1a shows the excitation spectra of pyrene at various $EC_{0.04}$-*g*-$PPEGMA_{12.8}$ copolymer concentrations in aqueous solutions. The concentration of pyrene in the aqueous solutions was fixed at 5.0×10^{-7} mol/L. The result indicates that the peak at 336 nm red shifted to 338 nm with the increase in copolymer concentration. The intensity ratio of I_{336}/I_{338} of every pyrene excitation spectra versus the logarithm of corresponding copolymer concentration is shown in Fig. 1b, by which

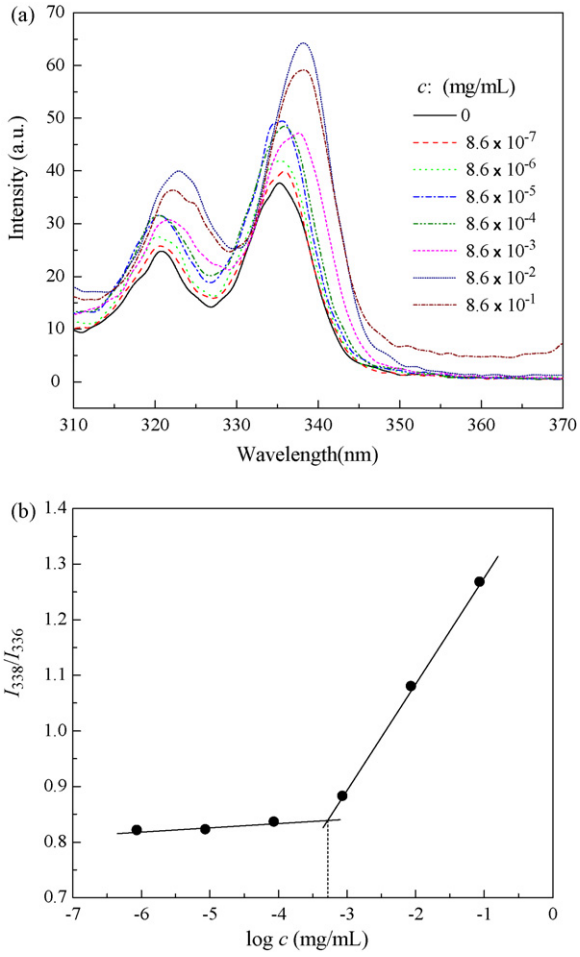

Fig. 1. The excitation spectra of pyrene in $EC_{0.04}$-*g*-$PPEGMA_{12.8}$ solution with different copolymer concentration (a) and the changes in the I_{336}/I_{338} intensity ratios from pyrene excitation spectra as a function of graft copolymer concentration (b).

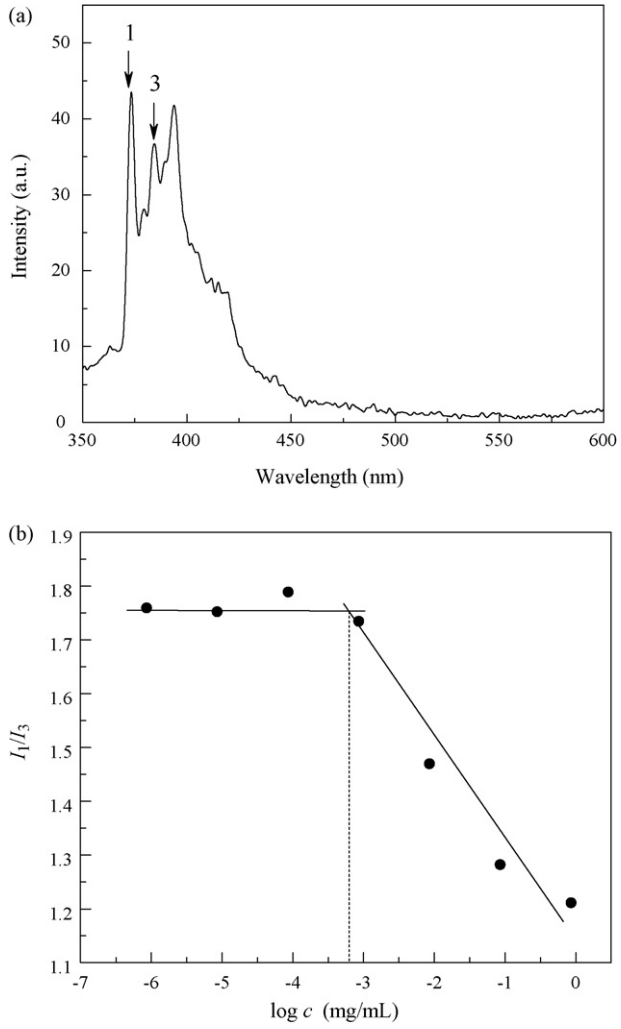

Fig. 2. Typical emission spectra of pyrene in graft copolymer aqueous solution (a) and plots of the intensity ratio of I_1/I_3 ratio of pyrene emission spectra as a function of graft copolymer concentration (b).

the CMC was determined at around 5×10^{-4} mg/mL for $EC_{0.04}$-*g*-$PPEGMA_{12.8}$.

The CMC of EC-*g*-PPEGMA in aqueous solution is also determined from the fluorescence intensity ratio of the first to that of the third peaks I_1/I_3. The fluorescence intensity ratio of the first to the third peaks I_1/I_3, depends on the environment of pyrene molecules, specifically the solute solvent interactions and/or the effective dielectric constant of the solvent (Kalyanasundaram & Thomas, 1977). The decrease of the environment polarity induces the decrease of the value of I_1/I_3 (Honda, Itagaki, Takeda, & Endo, 2002; Kalyanasundaram & Thomas, 1977). Fig. 2a shows the typical emission spectra of pyrene in EC-*g*-PPEGMA copolymer aqueous solution and the I_1/I_3 ratio as a function of EC-*g*-PPEGMA concentration is shown in Fig. 2b, which also indicates that the CMC for $EC_{0.04}$-*g*-$PPEGMA_{12.8}$ in aqueous solution is 5×10^{-4} mg/mL.

All the excitation spectra and emission spectra prove that the amphiphilic $EC_{0.04}$-*g*-$PPEGMA_{12.8}$ copolymer show the low CMC about 5×10^{-4} mg/mL. It can self-assemble into micelles in aqueous phase when the concentration of the EC-*g*-PPEGMA is higher than the CMC in which the hydrophobic EC backbones are collapsed to form the core stabilized with the hydrophilic side PPEGMA chains upon the CMC of about 5×10^{-4} mg/mL. Pyrene tends to transfer from the water solution to the micelles when the micellization happened and the pyrene could exist in the hydrophobic core of the EC backbones of the micelle. Therefore, if the micelles formed upon the concentration of CMC, the hydrophobic pyrene would locate in the EC hydrophobic core of the micelle. As a result, the hydrophobic core may be used as a reservoir of hydrophobic drugs and the micelles can be used as a drug delivery system.

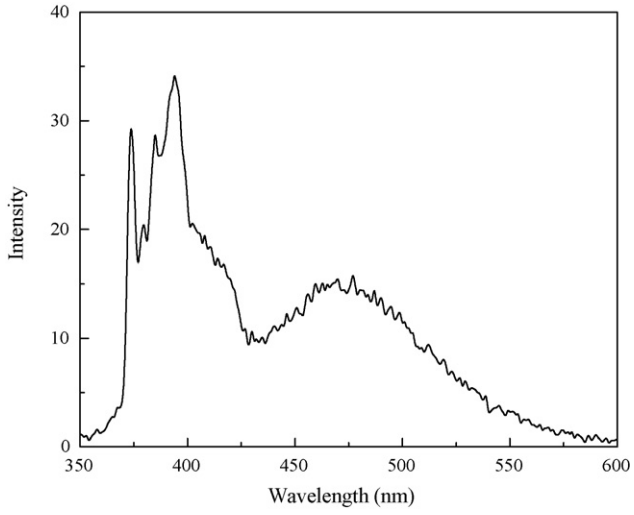

Fig. 3. Fluorescence spectrum of $EC_{0.04}$-*g*-$PPEGMA_{12.8}$ pyrene-loaded micelles. The mass feeding ratio of graft copolymer to pyrene in the preparation of pyrene-loading micelles M_{polym}/M_{py} is 5:1 and the EC-*g*-PPEGMA copolymer concentration is 1 mg/mL.

3.2. Preparation and characterization of the pyrene-loading micelles

Pyrene has also been used as a model drug in controlled release (Chen, He, Tang, & Yan, 2008b; Ma, Zhang, Song, Wang, & Zhang, 2005). In this work, the pyrene-loading micelle was prepared by dialysis method. The fluorescence spectrum of pyrene-loading micelle is shown in Fig. 3. In the research of pyrene micellization behavior, trace amount of pyrene was used as the probe to probe the micellization behavior of EC-*g*-PPEGMA and existed in unimolecule condition. However, in the pyrene-loading micelle, a large amount of pyrene aggregates in the hydrophobic core of the micelle, a excited pyrene can form excimer upon encounter with a ground-state pyrene monomer (Chen, 2005). The excimer peak of pyrene at 480 nm also proves that pyrene aggregates in the hydrophobic core of the micelle.

To contrast blank micelle and pyrene-loading micelle, the blank micelles and pyrene-loading micelles of $EC_{0.04}$-*g*-$PPEGMA_{12.8}$ were characterized by DLS. Fig. 4 shows the hydrodynamic radius ($\langle R_h \rangle$) distribution of the pure micelles and pyrene-loaded micelles of the graft copolymer $EC_{0.04}$-*g*-$PPEGMA_{12.8}$ and $EC_{0.04}$-*g*-$PPEGMA_{6.6}$. The results indicate that all the micelles have the good unimodal size distribution. For the sample $EC_{0.04}$-*g*-$PPEGMA_{12.8}$, the average hydrodynamic radius $\langle R_h \rangle$ of the pure micelle is about 31 nm, while $\langle R_h \rangle$ of the pyrene-loaded micelles is 52 and 62 nm for pyrene content of 2.8% and 4.1%, respectively, which is much larger than that of the pure micelles. For the sample $EC_{0.04}$-*g*-$PPEGMA_{12.8}$, the average hydrodynamic radius $\langle R_h \rangle$ of the pure micelle is about 54 nm and $\langle R_h \rangle$ of the pyrene-loaded micelles is 156 nm for pyrene content of 4.2%. The increase of the $\langle R_h \rangle$ of the micelle with increasing pyrene content results from the solubilized pyrene in the hydrophobic core of the micelle. Moreover, whatever the blank micelles and pyrene-loading micelles, the side chain length of the graft copolymer affects the $\langle R_h \rangle$ of the micelles obviously. The $\langle R_h \rangle$ of micelles of $EC_{0.04}$-*g*-$PPEGMA_{6.6}$ is larger than the micelles of $EC_{0.04}$-*g*-$PPEGMA_{12.8}$. Therefore

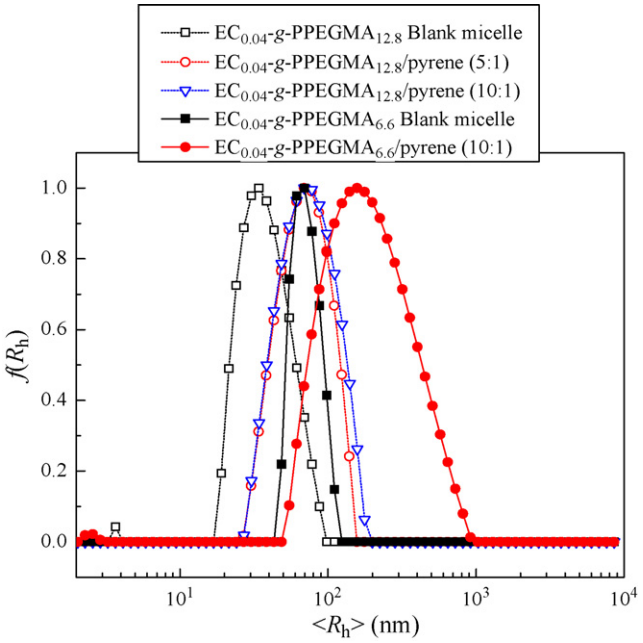

Fig. 4. Hydrodynamic radius distribution of the self-assembled blank micelle and pyrene-loading micelle at copolymer to pyrene ration of 5:1 and 10:1. All the measurements were carried out at the scattering angle of 90° and the temperature of 25 °C.

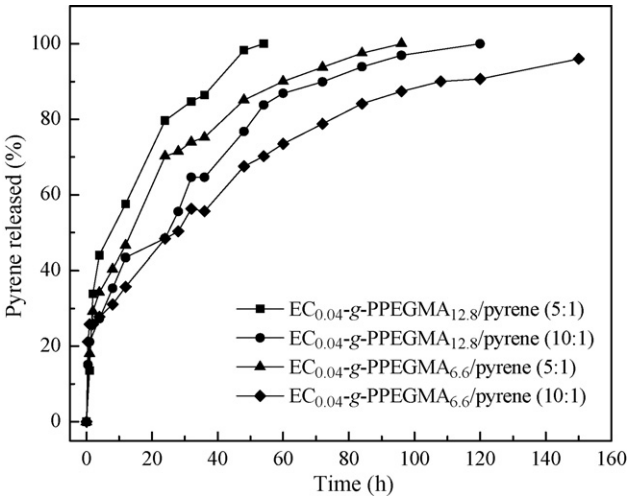

Fig. 5. The release profile of pyrene from the EC-*g*-PPEGMA micelles to phosphate buffer solution (PBS) (pH = 7.4) as a function of time at 37 °C.

the $EC_{0.04}$-*g*-$PPEGMA_{6.6}$ micelles contains more molecules of copolymer.

3.3. Pyrene-loading and release behavior of EC-*g*-PPEGMA micelles

The loading capacity and probe content was determined by working curve of pyrene in THF. The loading capacity and probe content of pyrene in the EC-*g*-PPEGMA micelles are listed in Table 1 at different conditions. The results indicate that the copolymers with lower graft density or shorter side chains have a higher loading efficiency and probe content, which attributes to the relatively higher content of hydrophobic EC backbone that has a better compatibility with pyrene at lower graft density. Moreover, higher graft density is the dominant fact on the loading efficacy and probe content than the side chain length. For example, the graft copolymers $EC_{0.15}$-*g*-$PPEGMA_{13.4}$ and $EC_{0.04}$-*g*-$PPEGMA_{12.8}$ with almost the same side chain length and different graft density showed obvious difference in the loading efficiency and probe content which may attribute to the higher flexibility, hydrophobicity and compatibility with pyrene for the EC backbone chains at lower DS.

Moreover, the loading efficiency also depends on the feeding ratio of graft copolymer to pyrene. For the graft copolymer of $EC_{0.04}$-*g*-$PPEGMA_{6.6}$ when the feeding ratio of graft copolymer to pyrene is changed from 5:1 to 10:1, the loading efficiency is increased from 17.7% to 24.4%. For the copolymer of $EC_{0.04}$-*g*-$PPEGMA_{12.8}$, the loading efficiency is increased from 16.3% to 28.3% when the feeding ratio of copolymer to pyrene is changed from 5:1 to 10:1. However, the increase in the feeding ratio of graft copolymer to pyrene has no obvious effect on the loading capacity in the micelles. This is due to that high proportion of polymer to pyrene corresponds to more micelles, that is more carriers for loading pyrene. Therefore, the loading efficiency increases with increasing in the polymer to pyrene ratio. However, loading capacity in the micelles was mainly determined by the structure and the property of the graft copolymer and partition coefficient of pyrene in the micelles (Lim Soo, Luo, Maysinger, & Eisenberg, 2002). As a result, the increase in the feeding ratio of graft copolymer have obvious effect on loading efficiency but no obvious effect on loading capacity of the micelles.

The release of pyrene from copolymer micelles (the average graft density of 0.04) with different graft length and ratio of W_{polym}/W_{py} was investigated in PBS solutions at 37 °C under constant stirring. The release of pyrene to the PBS solution as a function of time is shown in Fig. 5. When the pyrene-loaded micelles was dialyzed against PBS solution, pyrene will diffuse into the PBS solution due to concentration gradient. All pyrene-loaded micelles show a two-step release profile, i.e. an initial burst release in the 1st hour and then a sustained release for a long time. The burst release of pyrene may be caused by the diffusion of absorbed pyrene from the hydrophilic corona of the micelle and then the followed sustained release may be dominated by the pyrene from the hydrophobic core of the micelles. The pyrene in the micelle of $EC_{0.04}$-*g*-$PPEGMA_{6.6}$ showed a slower release than that in the micelle of $EC_{0.04}$-*g*-$PPEGMA_{12.8}$, which is due to the higher pyrene probe content in the $EC_{0.04}$-*g*-$PPEGMA_{6.6}$ micelles (Jeong et al., 2006). Furthermore the release rate can be controlled by changing the ratio of the copolymer to the pyrene for a graft copolymer with same graft length. The higher ratio leads to the slower release rates, which is consistent with literature (Lim Soo et al., 2002; Wang et al., 2008). The results mentioned above suggest that EC-*g*-PPEGMA copolymers might be used as a good carrier material for the sustained release of hydrophobic drugs.

4. Conclusion

The EC-*g*-PPEGMA copolymers demonstrated the low critical micelle concentration (CMC), i.e., 5×10^{-4} mg/mL. The release of pyrene from the EC-*g*-PPEGMA copolymer micelles was sustained in phosphate buffer solution (PBS) (pH = 7.4) at 37 °C. The pyrene in the micelles of the copolymers with shorter side chain length and in the system with the higher ratio of the copolymer to the pyrene showed a lower release rate. The EC-*g*-PPEGMA copolymers showed a potential application in controlled drug delivery systems.

Acknowledgements

The financial support of the National Natural Science Foundation of China (Grant Nos. 20974114, 20774105, and 50821062) and the Knowledge Innovation Program of the Chinese Academy of Sciences (Grant No. KJCX2-YW-H19) is greatly appreciated.

References

Allen, C., Maysinger, D., & Eisenberg, A. (1999). Nano-engineering block copolymer aggregates for drug delivery. *Colloids and Surfaces B Biointerfaces*, *16*, 3–27.

Bajpai, A. K., Shukla, S. K., Bhanu, S., & Kankane, S. (2008). Responsive polymers in controlled drug delivery. *Progress in Polymer Science*, *33*, 1088–1118.

Bian, F. L., Jia, L. X., Yu, W., & Liu, M. Z. (2009). Self-assembled micelles of *N*-phthaloylchitosan-*g*-polyvinylpyrrolidone for drug delivery. *Carbohydrate Polymers*, *76*, 454–459.

Biswal, D. R., & Singh, R. P. (2006). Flocculation studies based on water-soluble polymers of grafted carboxymethyl cellulose and polyacrylamide. *Journal of Applied Polymer Science*, *102*, 1000–1007.

CancheEscamilla, G., RodriguezTrujillo, G., HerreraFranco, P. J., Mendizabal, E., & Puig, J. E. (1997). Preparation and characterization of henequen cellulose grafted with methyl methacrylate and its application in composites. *Journal of Applied Polymer Science*, *66*, 339–346.

Carlmark, A., & Malmstrom, E. (2002). Atom transfer radical polymerization from cellulose fibers at ambient temperature. *Journal of the American Chemical Society*, *124*, 900–901.

Chen, A. L., Ni, H. C., Wang, L. F., & Chen, J. S. (2008). Biodegradable amphiphilic copolymers based on poly(ε-caprolactone)-graft chondroitin sulfate as drug carriers. *Biomacromolecules*, *9*, 2447–2457.

Chen, H. M., He, J. H., Tang, H. M., & Yan, C. X. (2008). Porous silica nanocapsules and nanospheres: Dynamic self-assembly synthesis and application in controlled release. *Chemistry of Materials*, *20*, 5894–5900.

Chen, P. (2005). *Molecular interfacial phenomena of polymers and biopolymers*. Cambridge: Woodhead Publishing Ltd.

Discher, D. E., & Eisenberg, A. (2002). Polymer vesicles. *Science*, *297*, 967–973.

Dong, H. Q., Xu, Q., Li, Y. Y., Mo, S. B., Cai, S. J., & Liu, L. J. (2008). The synthesis of biodegradable graft copolymer cellulose-graft-poly(L-lactide) and the study of its controlled drug release. *Colloids and Surfaces B Biointerfaces*, *66*, 26–33.

Duhamel, J. (2005). Pyrene fluorescence to study polymeric systems. In P. Chen (Ed.), *Molecular interfacial phenomena of polymers and biopolymers* (pp. 214–248). Cambridge, England: Woodhead Publishing Ltd.

Fleet, R., McLeary, J. B., Grumel, V., Weber, W. G., Matahwa, H., & Sanderson, R. D. (2008). RAFT mediated polysaccharide copolymers. *European Polymer Journal*, *44*, 2899–2911.

Guclu, G., Gurdag, G., & Ozgumus, S. (2003). Competitive removal of heavy metal ions by cellulose graft copolymers. *Journal of Applied Polymer Science*, *90*, 2034–2039.

Hebeish, A., Waly, A., Abdel-Mohdy, F. A., & Aly, A. S. (1997). Synthesis and characterization of cellulose ion exchangers. 1. Polymerization of glycidyl methacrylate, dimethylaminoethyl methacrylate, and acrylic acid with cotton cellulose using thiocarbonate-H_2O_2 redox system. *Journal of Applied Polymer Science*, *66*, 1029–1037.

Honda, C., Itagaki, M., Takeda, R., & Endo, K. (2002). Solubilization of pyrene in CnE7 micelles. *Langmuir*, *18*, 1999–2003.

Ifuku, S., & Kadla, J. F. (2008). Preparation of a thermosensitive highly regioselective cellulose/*N*-isopropylacrylamide copolymer through atom transfer radical polymerization. *Biomacromolecules*, *9*, 3308–3313.

Jeong, Y. I., Na, H. S., Oh, J. S., Choi, K. C., Song, C. E., & Lee, H. C. (2006). Adriamycin release from self-assembling nanospheres of poly(DL-lactide-*co*-glycolide)-grafted pullulan. *International Journal of Pharmaceutics*, *322*, 154–160.

Jun, Y. J., Toti, U. S., Kim, H. Y., Yu, J. Y., Jeong, B., Jun, M. J., et al. (2006). Thermoresponsive micelles from oligopeptide-grafted cyclotriphosphazenes. *Angewandte Chemie-International Edition*, *45*, 6173–6176.

Kabanov, A. V., & Alakhov, V. Y. (2002). Pluronic (R) block copolymers in drug delivery: From micellar nanocontainers to biological response modifiers. *Critical Reviews in Therapeutic Drug Carrier Systems*, *19*, 1–72.

Kalyanasundaram, K., & Thomas, J. K. (1977). Environmental effects on vibronic band intensities in pyrene monomer fluorescence and their application in studies of micellar systems. *Journal of the American Chemical Society*, *99*, 2039–2044.

Kang, H., Liu, W., He, B., Shen, D., Ma, L., & Huang, Y. (2006). Synthesis of amphiphilic ethyl cellulose grafting poly(acrylic acid) copolymers and their self-assembly morphologies in water. *Polymer*, *47*, 7927–7934.

Kang, H. L., Liu, W. Y., Liu, R. G., & Huang, Y. (2008). A novel, amphiphilic ethyl cellulose grafting copolymer with poly(2-hydroxyethyl methacrylate) side chains and its micellization. *Macromolecular Chemistry and Physics*, *209*, 424–430.

Kataoka, K., Harada, A., & Nagasaki, Y. (2001). Block copolymer micelles for drug delivery: Design, characterization and biological significance. *Advanced Drug Delivery Reviews*, *47*, 113–131.

Kim, C., Lee, S. C., Shin, J. H., Yoon, J.-S., Kwon, I. C., & Jeong, S. Y. (2000). Amphiphilic diblock copolymers based on poly(2-ethyl-2-oxazoline) and poly(1,3-trimethylene carbonate): Synthesis and micellar characteristics. *Macromolecules*, *33*, 7448–7452.

Kwon, G. S. (2003). Polymeric micelles for delivery of poorly water-soluble compounds. *Critical Reviews in Therapeutic Drug Carrier Systems*, *20*, 357–403.

Kwon, G. S., & Okano, T. (1996). Polymeric micelles as new drug carriers. *Advanced Drug Delivery Reviews*, *21*, 107–116.

Li, Y. X., Liu, R. G., & Huang, Y. (2008). Synthesis and phase transition of cellulose-graft-poly(ethylene glycol) copolymers. *Journal of Applied Polymer Science*, *110*, 1797–1803.

Li, Y. X., Liu, R. G., Liu, W. Y., Kang, H. L., Wu, M., & Huang, Y. (2008). Synthesis, self-assembly, and thermosensitive properties of ethyl cellulose-*g*-P(PEGMA) amphiphilic copolymers. *Journal of Polymer Science Part A-Polymer Chemistry*, *46*, 6907–6915.

Lim Soo, P., Luo, L., Maysinger, D., & Eisenberg, A. (2002). Incorporation and release of hydrophobic probes in biocompatible polycaprolactone-*block*-poly(ethylene oxide) micelles: Implications for drug delivery. *Langmuir*, *18*, 9996–10004.

Lindqvist, J., Nystrom, D., Ostmark, E., Antoni, P., Carlmark, A., Johansson, M., et al. (2008). Intelligent dual-responsive cellulose surfaces via surface-initiated ATRP. *Biomacromolecules*, *9*, 2139–2145.

Liu, X. M., Pramoda, K. P., Yang, Y. Y., Chow, S. Y., & He, C. B. (2004). Cholesteryl-grafted functional amphiphilic poly(*N*-isopropylacrylamide-*co*-*N*-hydroxylmethylacrylamide): Synthesis, temperaturesensitivity, self-assembly and encapsulation of a hydrophobic agent. *Biomaterials*, *25*, 2619–2628.

Liu, Y. L., Lin, G. C., & Wu, C. S. (2008). Preparation of polysulfone-*g*-poly(*N*-isopropylacrylamide) graft copolymers through atom transfer radical polymerization and formation of temperature-responsive nanoparticles. *Journal of Polymer Science Part A-Polymer Chemistry*, *46*, 4756–4765.

Ma, N., Zhang, H., Song, B., Wang, Z., & Zhang, X. (2005). Polymer micelles as building blocks for layer-by-layer assembly: An approach for incorporation and controlled release of water-insoluble dyes. *Chemistry of Materials*, *17*, 5065–5069.

Meng, T., Gao, X., Zhang, J., Yuan, J. Y., Zhang, Y. Z., & He, J. S. (2009). Graft copolymers prepared by atom transfer radical polymerization (ATRP) from cellulose. *Polymer*, *50*, 447–454.

Moad, G., Rizzardo, E., & Thang, S. H. (2008). Radical addition-fragmentation chemistry in polymer synthesis. *Polymer*, *49*, 1079–1131.

Ostmark, E., Harrisson, S., Wooley, K. L., & Malmstrom, E. E. (2007). Comb polymers prepared by ATRP from hydroxypropyl cellulose. *Biomacromolecules*, *8*, 1138–1148.

Pourjavadi, A., & Mahdavinia, G. R. (2005). Superabsorbency and swelling behaviour of partially hydrolyzed carboxymethylcellulose-*g*-PAAm hydrogels. *Journal of Polymer Materials*, *22*, 235–243.

Rajam, S., & Ho, C. C. (2006). Graft coupling of PEO to mixed cellulose esters microfiltration membranes by UV irradiation. *Journal of Membrane Science*, *281*, 211–218.

Rapoport, N. (2007). Physical stimuli-responsive polymeric micelles for anti-cancer drug delivery. *Progress in Polymer Science*, *32*, 962–990.

Riley, T., Govender, T., Stolnik, S., Xiong, C. D., Garnett, M. C., Illum, L., et al. (1999). Colloidal stability and drug incorporation aspects of micellar-like PLA-PEG nanoparticles. *Colloids and Surfaces B Biointerfaces*, *16*, 147–159.

Roy, D., Guthrie, J. T., & Perrier, S. (2008). Synthesis of natural–synthetic hybrid materials from cellulose via the RAFT process. *Soft Matter*, *4*, 145–155.

Savic, R., Eisenberg, A., & Maysinger, D. (2006). Block copolymer micelles as delivery vehicles of hydrophobic drugs: Micelle-cell interactions. *Journal of Drug Targeting*, *14*, 343–355.

Shen, D., Yu, H., & Huang, Y. (2006). Synthesis of graft copolymer of ethyl cellulose through living polymerization and its self-assembly. *Cellulose*, *13*, 235–244.

Shen, D. W., & Yong, H. (2004). The synthesis of CDA-*g*-PMMA copolymers through atom transfer radical polymerization. *Polymer*, *45*, 7091–7097.

Shen, D. W., Yu, H., & Huang, Y. (2005). Densely grafting copolymers of ethyl cellulose through atom transfer radical polymerization. *Journal of Polymer Science Part A-Polymer Chemistry*, *43*, 4099–4108.

Srivastava, A., & Behari, K. (2006). Studies on graft copolymerization of *N*-vinyl-2-pyrrolidone on to carboxymethylcellulose (sodium salt) and metal ion sorption behavior. *Journal of Macromolecular Science Part A-Pure and Applied Chemistry*, *43*, 1065–1081.

Sui, X. F., Yuan, J. Y., Zhou, M., Zhang, J., Yang, H. J., Yuan, W. Z., et al. (2008). Synthesis of cellulose-*graft*-poly(*N*,*N*-dimethylamino-2-ethyl methacrylate) copolymers via homogeneous ATRP and their aggregates in aqueous media. *Biomacromolecules*, *9*, 2615–2620.

Waly, A., Abdel-Mohdy, F. A., Aly, A. S., & Hebeish, A. (1998). Synthesis and characterization of cellulose ion exchanger. II. Pilot scale and utilization in dye heavy metal removal. *Journal of Applied Polymer Science*, *68*, 2151–2157.

Wang, J., Tang, F. S., Li, F., Lin, J., Zhang, Y. H., Du, L. F., et al. (2008). The amphiphilic self-assembling peptide EAK16-I as a potential hydrophobic drug carrier. *Journal of Nanomaterials*, 516286.

Wang, J. S., & Matyjaszewski, K. (1995). Controlled/"living" radical polymerization. Atom transfer radical polymerization in the presence of transition-metal complexes. *Journal of the American Chemical Society*, *117*, 5614–5615.

Wei, Y. P., Cheng, F., Hou, G., & Sun, S. F. (2008). Amphiphilic cellulose: Surface activity and aqueous self-assembly into nano-sized polymeric micelles. *Reactive & Functional Polymers*, *68*, 981–989.

Winnik, F. M. (1993). Photophysics of preassociated pyrenes in aqueous polymer solutions and in other organized media. *Chemical Reviews*, *93*, 587–614.

Yan, Q., Yuan, J. Y., Zhang, F. B., Sui, X. F., Xie, X. M., Yin, Y. W., et al. (2009). Cellulose-based dual graft molecular brushes as potential drug nanocarriers: Stimulus-responsive micelles, self-assembled phase transition behavior, and tunable crystalline morphologies. *Biomacromolecules*, *10*, 2033–2042.

Yu, H. F., Fu, G. Q., Zhao, J. C., Liu, L., & He, B. L. (2006). Synthesis and in vitro sorption properties of PAA-grafted cellulose beads for selective binding of LDL. *Artificial Cells Blood Substitutes and Biotechnology*, *34*, 501–513.

Zhang, L. M., Tan, Y. B., & Li, Z. M. (1999). Application of a new family of amphoteric cellulose-based graft copolymers as drilling-mud additives. *Colloid and Polymer Science*, *277*, 1001–1004.

Zhang, X. W., Zhu, X. Q., Ke, F. Y., Ye, L., Chen, E. Q., Zhang, A. Y., et al. (2009). Preparation and self-assembly of amphiphilic triblock copolymers with polyrotaxane as a middle block and their application as carrier for the controlled release of amphotericin B. *Polymer*, *50*, 4343–4351.